Fully bio-sourced catalyst-free covalent adaptable networks from epoxidized soybean oil and L-tartaric acid

Neymara C Nepomuceno, Camille Bakkali-Hassani, Renate Wellen, Sylvain Caillol, Claire Negrell

Fully bio-sourced catalyst-free Covalent Adaptable Networks from epoxidized soybean oil and L-tartaric acid

Neymara C. Nepomuceno[a*], Camille Bakkali-Hassani[a], Renate Wellen[b], Sylvain Caillol[a], Claire Negrell[a*]

[a]Institut Charles Gerhardt Montpellier – ICGM – Université de Montpellier, CNRS, ENSCM, Montpellier, France

[b] Universidade Federal da Paraíba – UFPB – João Pessoa, Brazil

***Corresponding Authors: Claire.negrell@enscm.fr and neymara.cavalcante@certbio.ufcg.edu.br**

Abstract: Epoxidized vegetable oil (EVO)-based epoxy systems offer a promising avenue for replacing non-recyclable petroleum-based thermoset elastomers. Looking towards future prospects, they also hold potential to evolve into sustainable covalent adaptable networks (CANs). Typically, transesterification-based CANs require catalysts to achieve crosslinked structures that are reprocessable at relatively high temperatures (T ≥ 150°C). In this study, epoxidized soybean oil (ESBO) was cross-linked with a eutectic hardener composed of L-tartaric acid (TAR) and ethyl lactate (in an aqueous solution), resulting in the development of a fully bio-based 3D covalent network capable of reprocessing without the need for an exogenous catalyst. In addition, it was demonstrated that the peculiar structure of L-tartaric acid, with -OH groups linked to its backbone, plays a prominent role in the reactivity of the system. These free hydroxyl functions facilitate both the ring-opening of epoxides and transesterification reactions, thus enhancing both curing and covalent exchange kinetics.

Keywords: epoxidized vegetable oils, epoxy resins, tartaric acid, covalent adaptable network.

Introduction:

The growing concern for sustainability and efficient management of plastic waste has spurred significant interest in developing new strategies for polymer recycling, especially regarding those deemed thermosetting, which pose specific challenges in the process. Thermosetting polymeric materials are possibly one of the most versatile

engineered materials that find a wide variety of applications due to their excellent thermal stability, mechanical properties, and chemical resistance [1]. Nonetheless, the permanent chemically crosslinked structure of thermoset is also accompanied by major drawbacks for recycling purposes. The network topology prevents both abilities to flow and to be reprocessed thus limiting their effective reusability by conventional recycling approaches.

In this context, covalent adaptable networks (CANs) have emerged as a promising solution once they present intermediate characteristics between thermoplastics and thermosets polymers as first described in 2011 by Leibler's group [2]. Despite their innovative characteristics, the majority of CANs employed oil-based monomers [3,4]. As a typical example, epoxy-based thermosets and CANs generally use diglycidyl ether of bisphenol A (DGEBA) as epoxy monomer. Since they present higher glass transition temperatures (T_g) and are known for being rigid and though, but also, may be versatile in the development of elastomeric thermosets [5]. However, DGEBA epoxy systems are highly dependent of petrochemical resources, non-sustainable/renewable, and is also toxic [6]. Nonetheless, considerable efforts have been made to prepare and cure epoxy systems from biobased resources such as vegetable oils and naturally occurring acids [7].

Epoxidized vegetable oils are largely evaluated as green monomers for epoxy systems once they are easily accessible and sustainable. The forecast for soybean production has increased in recent years, and estimated production of 155 thousand metric tons by the largest producer of the grain alone (Brazil) [8]. Worldwide, soybean oil is the most produced in the world (396 million metric tons/year) and is used domestically and technologically (as lubricant during PVC processing) [9,10]. They present attractive features such as a high degree of functionality (unsaturation, epoxy functions, and ester groups in the same molecular structure), relatively low cost, making them promising candidates to generate fully biobased thermosets with inherent reprocessability and recyclability [11–14]. However, their in-chain oxirane groups exhibit lower reactivity, leading to low Tg and poor mechanical properties when compared to petrochemical monomers bearing epoxy glycidyl functions [15–18]. Natural occurring acids (citric, succinic, tartaric, and sebacic acids, for example) stand

out as curing agent candidates for epoxy systems targeting vitrimeric properties but present some limitations such as high melting temperature, low solubility in EVOs and in some cases unstable at high temperature (decarboxylation of citric acid) [19,20]. In an ideal formulation, the melting temperature of the acid should be below the curing temperature, to ensure the complete dissolution of the acid groups in the epoxy monomer before the onset of curing reactions, which usually occurs between 120-150°C.

Some approaches were reported in the literature to overcome those problems, Altuna *et al*. used citric acid (CA) as a hardener for epoxidized soybean oil (ESO) without the addition of catalysts or harmful solvents by simply dissolving CA in water. Despite having reported a homogeneous material with potential reprocessability, the use of water as a liquefier solvent can induce phase separation and side reaction with the epoxy group without creating crosslinked networks [21]. A similar methodology was used by Jie Li *et al.* to dissolve succinic acid (SuA) in ESO for CANs with decent reprocessability, but one step to promote evaporation of water was settled at 140°C for 1h, and at this temperature, some side reactions can take place during the formation of the network, which can compromise the final density of exchangeable linkages [22]. Another approach was the dissolution of citric acid in a low boiling point organic solvent (THF, 66°C), and used as hardener in epoxidized castor and linseed oils. But when the main objective is producing a fully biobased epoxy system, the use of such solvent is not attractive [23].

To deal with these adversities, the concept of eutectic hardeners (EH) was introduced by Tellers and collaborators and aims to promote a better route of use of carboxylic acids with higher melting temperatures in epoxy systems [24,25]. In their work, they successfully used a green solvent (ethyl lactate-EL), as a liquefier for citric and malic acid, lowering its T_m and activating it in curing reaction epoxidized linseed oil (ELO). The same procedure was employed for tartaric acid, without achieving the same results due to side reactions. Among naturally occurring acids, L-tartaric acid emerges as an interesting hardener for epoxy-acid systems, as it is one of the main residues of the winery industry and its widely used in the food industry [26–28]. Furthermore, it presents attractive reactivity caused by its low pKa, but also extra OH groups with

controlled stereochemistry in the structure that can be attractive for the development of CANs [29].

Herein, aiming the use of L-tartaric acid (TAR) as a hardener for epoxidized soybean oil (ESBO) in the development of fully bio-sourced epoxy systems (ESBOTAR), the concept of eutectic hardeners (EH) was applied with some modifications. In the present work, we successfully achieved an EH dissolving L-tartaric acid in an aqueous solution of ethyl lactate. The molar ratio between L-tartaric acid and ESBO was varied in 0.3, 0.5, 0.7, and 0.8 carboxylic/epoxy groups ([COOH]/[oxirane] ratio) and their influence in the physical-chemical characteristics and thermo-mechanical properties of the obtained materials was evaluated. By combining rheological characterizations (stress relaxation experiments), reprocessing tests, and the synthesis of a "blank prototype" using succinic acid hardener, we demonstrated that the presence of extra hydroxyl functions and their specific distribution offered to this fully biobased material good reactivity and reprocessability without the introduction of an exogenous catalyst.

Results and discussion

Polymerization reaction and curing mechanisms.

To obtain the eutectic hardener, our group suggested a new approach for the dissolution of tartaric acid, which consists of an aqueous solution of ethyl lactate combined with low processing temperatures (lower than 100°C). After several tests, the dissolution of L-tartaric acid was achieved after 5 min at 80°C in an ethyl lactate aqueous solution (C= 0.72 g/mL) and keeping the initial molar ratio used in Tellers work's (R=1 COOH/ethyl lactate)[25]. After that, the solution was directly mixed with epoxidized soybean oil (ESBO) at 80°C for 1 h. After the mixing protocol, the final formulation presented as homogeneous and stable, *i.e*., no phase separation or crystallization of tartaric acid was observed. The cured samples presented transparency and homogeneity, with the absence of bubbles or segregation of acid in the final sample, and with the increase in molar ratio of TAR, it can be noticed the intensification of a yellowish color (Figure 1 and SM2).

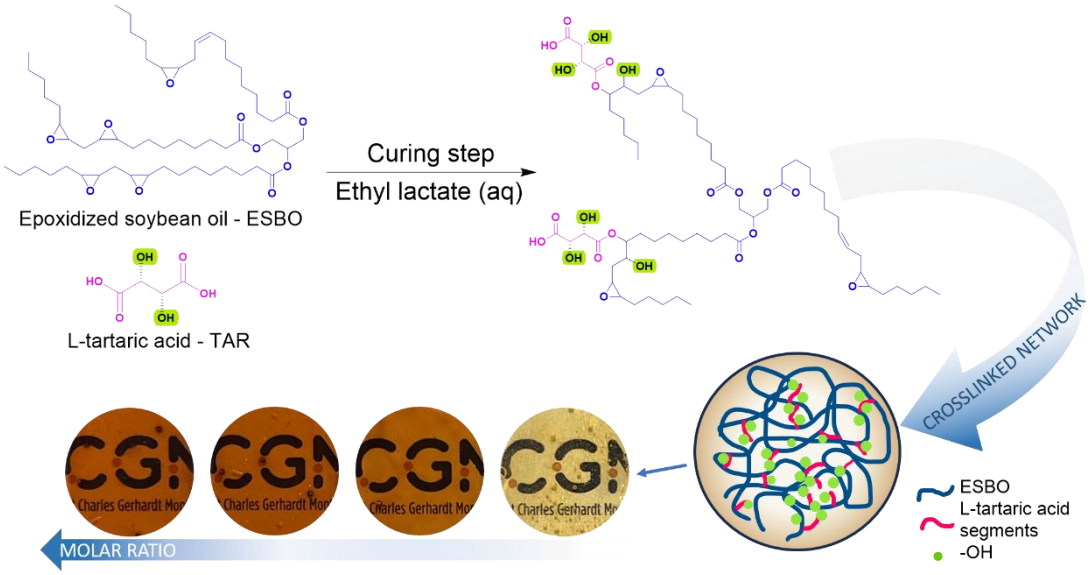

Figure 1 – Schematic representation of reaction between ESBO and L-tartaric acid (TAR) and cured ESBOTAR resins obtained after curing (with 1st step at 105°C for 4h and 2nd step at 130°C overnight).

Curing of ESBOTAR system analyzed by FT-IR studies.

FTIR spectroscopy was used to monitor the epoxy-acid reaction depending on the molar ratio employed for the curing (spectra of uncured and cured samples of ESBO and L-tartaric acid are presented in Figure S3, Supplementary material-SM). The dispersion of the acid in the medium is generally poor resulting in acid segregation and consequently incomplete reactions. In this system, due to the good stability of the eutectic hardener, the constant presence of reactive L-tartaric acid guarantees a homogeneous phase. This leads to good conversion of epoxy groups right after the mixing step (1h at 80°C) with values of 15, 30, 37, and 54% for R = 0.3, 0.5, 0.7, and 0.8 respectively. In all systems, no significant residual signals centered at around 840-820 cm^{-1}, related to the oxirane ring, were observed after the curing procedure, indicating successful ring-opening reactions. In the carbonyl region, a shift of the C=O stretching signal toward higher wavenumbers was observed, and a broad signal from 1680-1650 cm^{-1} that was related to the carbonyl from tartaric acid was shifted to 1740 cm^{-1} which is associated with C=O stretching from the esters formed in the crosslinked structure. A signal around 3500 cm^{-1} associated with OH stretching from the hydroxyl groups is

also discernable in the cured samples as expected with the formation of hydroxy ester moieties.

Surprisingly, regardless of the initial molar feed ratio, epoxy signature vibration bands exhibited similar absorbance values. Figure – 2a shows a kinetic FT-IR analysis (just the interval 1900-750 cm^{-1} was highlighted) done for ESBOTAR with molar ratio R = 0.7 at 130°C for 15 hours to bring a better understanding of the mechanism(s) involved during curing. The conversion plot presented in Figure 2b shows a first-order kinetic profile, this behavior is associated with homogeneous polymerization while zero-order kinetic was recorded in the case of biphasic (presence of acid crystals) [30]. In the region related to C=O stretching, as the reaction progresses, the formation of β-hydroxy-esters is evidenced by a shift towards higher wavenumbers (1730-1750 cm^{-1}). Simultaneously, in the region associated with the C-O-C stretching of the oxirane ring, it is possible to observe its decrease over time, until an apparent complete consumption of all oxirane groups.

A plausible explanation was the occurrence of etherification reactions which is normally accompanied by an increase of ether bands (C-O-C) around 1150 cm^{-1} but was not detected here. Glycidyl functions are more reactive than 1,2-disubstituted epoxies and can be subjected to homopolymerization[24], even so, in a non-catalyzed epoxy-acid, using phenyl glycidyl ether and hexanoic acid, conversions around 30 and 50% were only reached after 48h and 72h at 100°C, of reaction respectively and no homopolymerization was recorded [31]. To go further and better understand this behavior, we performed model molecular transformations in different conditions (acid monomers and initial feed ratio [COOH]/[oxirane]).

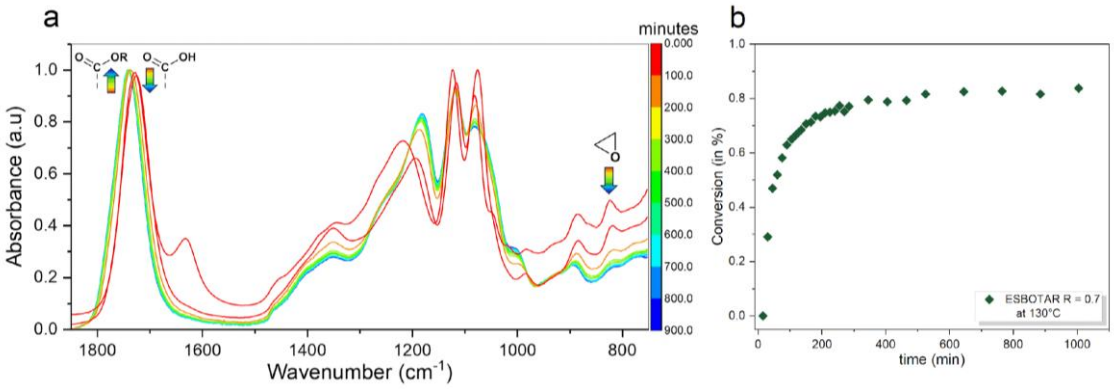

Figure 2 – Curing analysis by ATR-IR kinetic (130°C) of a selected formulation (R=0.7). Zoom on the region from 1850 to 750 cm^{-1} (left) and conversion in % of epoxy groups in function of time (right).

The reactivity of tartaric acid in this epoxy system was evaluated by molecular model reaction and compared with a similar acid which does not contain the extra hydroxyl functions. Epoxidized methyl oleate (EMO), L-tartaric (TAR), and succinic acid (SUC) were used as model molecules since they mimic the chemical functions of this epoxy-acid system, *i.e.* the in-chain epoxide groups founded in ESBO and the influence from -OH groups present in tartaric acid. The conversion of epoxy groups was evaluated by ^{1}H NMR, and the details are given in supplementary material. Around 90% of conversion was achieved after 1h of reaction (at 100°C) when L-tartaric acid was used in stoichiometric amounts ([COOH]=2[EMO]) although only 12% when succinic acid was employed in similar conditions (Figures SM 4, 5 and 6). The lower pKa of L-tartaric acid (pKa_1= 2.98 and pKa_2= 4.34) compared to succinic acid (pKa_1= 4.21 and pKa_2= 5.64) could explain the higher reactivity of TAR towards ring-opening of oxiranes (Figure – 3). Whilst, the literature on the ring-opening of epoxides by carboxylic acids activated by tertiary amine or heterocyclic bases is abundant and the mechanism well-described [32], only a few works performed the oxirane ring-opening with acids in a non-catalyzed process. In this particular case, the stronger the carboxylic acids seem to push the equilibrium towards the formation of the carboxylate anion (that further reacts with the epoxy ring) [33,34]. Even using a lower concentration of tartaric acid ([COOH]=4[EMO]), the consumption of epoxide group was relatively fast, proving a catalytic effect (Figure – SM7). The homopolymerization effect hypothesis was disregarded after evaluating the EMO under the same previous experimental

conditions, where epoxy consumption by ^{1}H NMR (Figure – SM8) and change in molar mass (Mw) by SEC were not observed (Figures – SM 9 and 10).

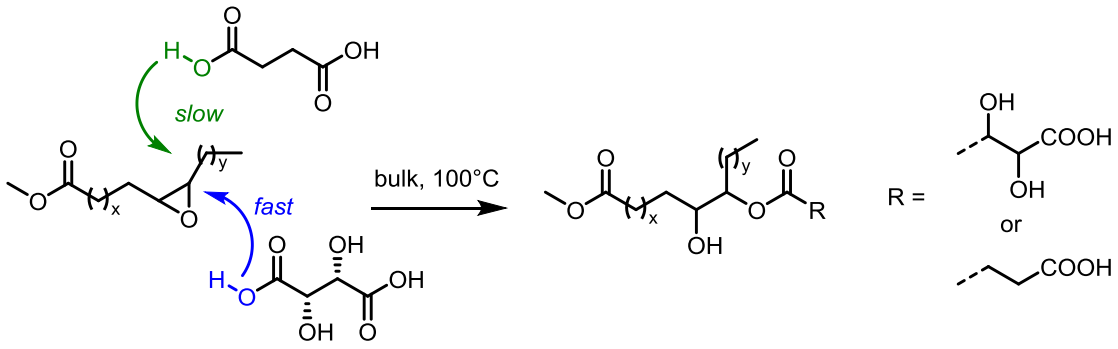

Figure 3- Molecular model reaction used to compare tartaric and succinic acid with epoxidized methyl oleate, reaction conditions: bulk, 100°C, up to 24h, [COOH] = 2 [EMO].

Influence of molar ratio in the thermal behavior of ESBOTAR system

The ESBO and ESBOTAR cured resins were investigated by DSC to analyze the effectiveness of the curing procedure and the glass transition temperature T_g as a function of the molar ratio. The curves are presented in Figures SM-11 and 11 and the values of enthalpy (for curing and after curing) and glass transition (T_g) are summarized in Table 2.

The curing and remaining enthalpies of curing were used to calculate the degree of curing (in %) and ranged from 95 to 98% for ESBOTAR formulations. These values are high, indicating that the curing and post-curing process used for the ESBOTAR system was efficient. They are also following the values obtained for the gel content and the conversion of epoxy groups, which will be presented further. Besides that, it was not observed in the interval of temperature from 25-200°C any exothermic event for the monomer which indicates that homopolymerization reactions of fatty acid in chain epoxides are not favorable under those conditions regardless of the molar ratio employed.

The T_g values increased from -17 to -13.7 °C when the molar ratio grew from 0.3 to 0.8 Furthermore, as presented in the work by Songqi Ma *et al.* epoxidized soyate sucrose cured with L-tartaric acid and malic acid presented higher glass transition

temperatures (T_g= 99°C and 66°C, respectively) than other carboxylic acids (T_g= 23 °C and 17°C for malonic and glutaric acid) and this can be explained by the presence of greater OH groups that can increase the hydrogen bonding of the cross-linked structure and, consequently increases the glass transition to higher temperatures, compared to materials made with other dicarboxylic acids, such as malonic or sebacic acids [20].

The T_g for the resins with epoxidized oils is expected to be lower compared to the commercial resins (usually around 50-110°C for DGEBA-based systems [6,35]) with does not make then suitable for replace this kind of epoxy systems. Otherwise, compared with other epoxidized vegetable oils, as an example of epoxidized linseed oil, epoxidized soybean oil usually presents the lowest values. Based on the literature, the lower T_g of ESBO is related to the lower equivalent epoxy weight (EEW) resulting in, after the crosslinking reactions, greater spacing between the aliphatic terminals of the fatty acid chains that make up the ESBO, while a greater EEW provides a greater density of these crosslinks. Therefore, an increase in T_g in epoxy systems with ESBO is highly dependent on the choice of curing agent of the presence of different functionalities, such as hydroxyl moieties [36–38].

Dynamic-mechanical analyses (DMA) were used to determine the storage modulus, mechanical loss factor (tan δ), and cross-linking density of cured samples and the results are listed in Table – 1 and presented in Figure- 4a, respectively.

The crosslinking density (υ, mol/cm^3) and molecular mass between crosslinking nodes is presented in Figure 4b. The increase of crosslinking density occurs concomitantly with the increase of molar ratio between COOH/epoxy following the pattern R = 0. 7 > 0.5 > 0.3 and decreases when R= 0.8 to similar values found in formulation with R=0.5. For the molar ratio equal to 0.5, 0.7, and 0.8 the rubbery plateau is almost overlapped, presenting values of E’ (at T = Tα + 50) equal to 1.1, 1.6, and 0.9 MPa, respectively. Related to the curve of storage modulus as a function of temperature, is possible to observe a plateau that persists more than 100°C for all the molar ratios ascribed to chain entanglement, which is indicative of a crosslinked material.. The storage modulus was also evaluated for the formulation ESBOTAR R=0.7 after the 3rd

reprocessing (Figures SM13-14)Supplementary material) and an increase of 5°C in the Tα was observed.

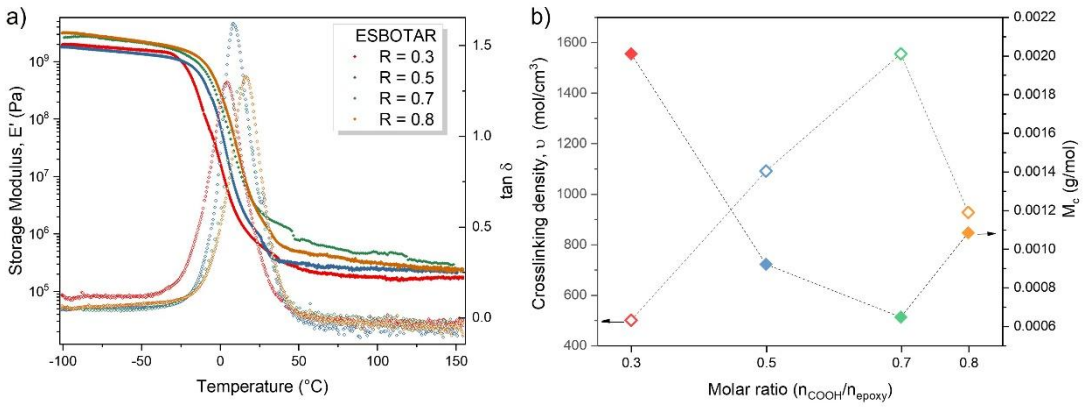

Figure 4 - (a) Storage modulus (E') as a function of temperature (°C) and mechanical loss factor tan δ as a function of temperature for ESBOTAR formulations varying molar ratio (R= n_{COOH}/n_{epoxy}) and (b) Crosslinking density (υ) and molecular weight between two dots of crosslinking (M_c) as a function of molar ratio R.

Table 1 - Glass transition calculated by (a) DMA and (b) DSC and the ΔH of curing and (c) remain cure (d)

Molar Ratio R = n_{COOH}/n_{epoxy}	T_α [a] (°C)	T_g [b] (°C)	ΔH [c] (kJ.mol^{-1})	ΔH [d] (J.g^{-1})
0.3	4.5	-17	83	1.7
0.5	9	-13	132	7
0.7	12	-11	140	4.8
0.8	16	- 13.7	166	5.7

The thermal stability of the cured samples was investigated by thermogravimetric analysis under a nitrogen atmosphere. Thermogravimetric (TG) and derivative thermogravimetric (DTG) curves are presented in Figure 5, and the corresponding data are listed in Table 2. The degradation temperatures at 5% mass loss ($T_{5\%}$) of the cured thermosets range from 262 to 287 °C and the temperature of maximum degradation (T_{max}) from 388 to 393°C. Observing the profile of DTG, the degradation events are quite similar for all the compositions. The first stage of mass loss occurs between room

temperature and 200°C and it is responsible for around 0.75-2% of mass loss, relative to humidity and lower mass compounds. The second stage (200-500°C) is due to the main process of thermal degradation, and it comprehends the successive break of ester linkages that makes the structure weaker until the complete disintegration of the crosslinked bulk material. As can be seen, a third and last step occurs at high temperatures, and it is related to thermo-oxidative degradations [39]. As reprocessing entails exposing materials to temperatures surpassing 150°C, it becomes essential to employ materials showcasing stability at these temperatures. Consequently, the thermal stability presented for the ESBOTAR system is indispensable to thwart degradation processes inherent in repetitive reprocessing cycles.

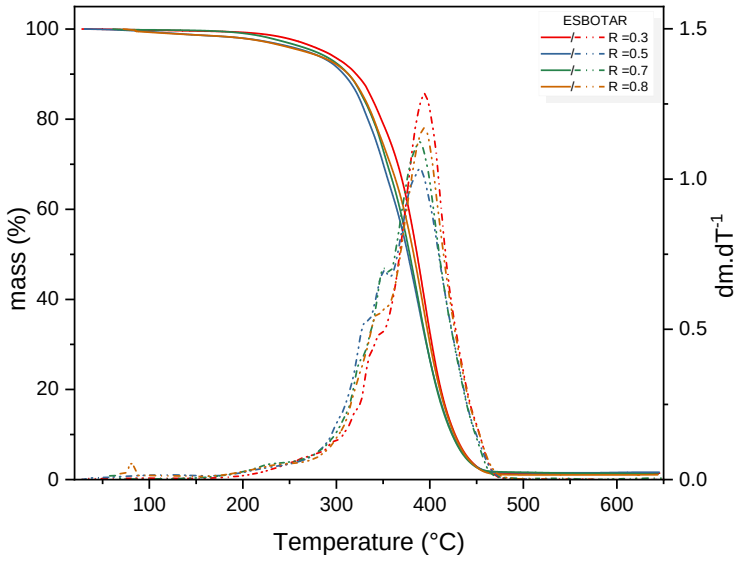

Figure 5 – TGA and DTG of ESBOTAR cured resins varying molar ratio from 0.3 to 0.8.

Table 2 - Temperatures at 5% mass loss ($T_{5\%}$), maximum temperature of thermal degradation (T_{max}), and mass loss (in %) at different stages of degradations of cured ESBOTAR samples.

Molar ratio	Temperatures		Mass loss (%)		Residue at 650°C
	$T_{5\%}$ mass loss (°C)	T_{max} (°C)	1st stage T~30- 200°C	2nd stage T~200-500°C	
R = 0.3	287	394	0.75	98	<1%
R = 0.5	268	389	2	97	
R = 0.7	278	388	1	98	

R = 0.8	267	393	2	97	

Gel content (%), conversion of epoxy groups, Swelling ratio (%) and chemical resistance.

To understand the influence of molar ratio in the structure of ESBOTAR resins, the gel content (%), conversion (α in %) of epoxide groups, swelling ratio (%) and chemical resistance were evaluated.

The conversion (α in %) of epoxide groups obtained were 96, 93, 93, and 94% for molar ratios equal to 0.3, 0.5, 0.7, and 0.8 respectively. Those results indicate the presence of a crosslinked network with the consumption of epoxy groups during the curing reaction.

As can be observed (Figure SM-15), the values of gel content for all the molar ratios were around 92 ± 2 % and 80± 2% when THF and DMF were used as solvents, respectively. These results are in accordance with those presented in the literature, which has a consensus that gel content greater than 80% indicates the presence of crosslinks. Songqi Ma et al. reported 94% of gel content with epoxidized sucrose soyate with L-tartaric acid at molar ratio R = 1 (acid/epoxy)[40]].

Regarding the results for the swelling ratio (Table SM 2), is possible to observe a significant decrease in the swelling ability with the evolution of the molar ratio, when apolar solvent is used (toluene), as expected. However, in the presence of DMF, we can observe that there are no significant changes in the degree of swelling for molar ratios from 0.3 to 0.7, which remains around 221±7 %, accompanied by an increase only for molar ratio 0.8 (to 276±8%). Besides that, the ESBOTAR system with R = 0.7 and 0.8 demonstrated not only a crosslinked network but also higher crosslinked density at the intermolecular level.

The chemical resistance was evaluated, and all molar ratios showed good stability in an acidic environment, remaining intact. However, in basic medium it was possible to observe the dissolution of all samples after one week (SFigure SM-16).

Those results are following crosslinked density calculated from dynamic mechanical analysis (DMA) and the tensile strength, which will be presented further in this paper.

Reprocessability of ESBOTAR resins

To go further in the evaluation of ESBOTAR as CANs, the material was reprocessed by compressing molding. Except for a molar ratio equal to 0.3, the other compositions were successfully reshaped after compression molding at 145°C with 4 tons overnight as presented in Figure SM17.

In terms of color, at the 1st cycle, the reprocessed samples did not present significant changes, but it is possible to notice the boundaries formed because of a gradient of color between the surface and interior from the original samples. Two other reprocessing cycles were performed and a change in color from yellowish to brownish was observed. A isothermal TGA (Figure SM 20) simulating the reprocessing condition was performed for the pristine samples in order to evaluate the formation of volatiles during the process, but only a loss of mass around 5-7% was observed and can be attributed to the humidity or even traces of solvent evaporation. The ATR-IR analysis of reprocessed sample surfaces revealed no discernible differences (as described in Supplementary FXX) in the C-O vibration range typically associated with the formation of ether bonds, spanning from 1050 to 1250 cm-1. Similarly, there were no notable distinctions in the intensity of OH vibration bands, approximately around 3500 cm-1. Ether formation have been reported through both the ring-opening polymerization (ROP) of epoxy moieties and dehydration reactions at high temperatures when utilizing glycidyl ether monomers. However, this phenomenon does not appear to occur with in-chain epoxy moieties [41]. Combining spectroscopic analysis, thermomechanical characterizations (DMA, TGA and tensile tests) and swelling tests demonstrated that no or low side reactions (oxidation, ether formation by dehydration or ROP of unreacted epoxides) are occurring under the reprocessing conditions (145°C, 4 tons, 12h) (Figures SM 19 – 21).

To follow the changes in microstructural level, the material was evaluated by infrared spectroscopy, degree of swelling and mechanical performance. As can be seen in the FT-IR spectra for the reprocessed samples (Figure SM19) neither the appearance of

new bands nor the modification of existing bands was observed, indicating that reprocessing can be accessed through associative mechanisms.

Figure 7 presents the average values of maximum tensile strength at break (MPa) and strain (%) for the pristine (0 RR) and reprocessed (RR) ESBOTAR resins as a function of molar ratios. As can be observed, the tensile strength grows with the increase of molar ratio and ranges between 0.004 and 0.9 MPa and the strain at break is between 97% and 147 %, when R = 0.3, 0.5 and 0.7 are taken into consideration. For the molar ratio R = 0.8, those values are around 0.6 MPa and 137 %, for tensile strength and strain, respectively.

Those values are in accordance with some epoxy resin systems that use epoxidized soybean oil and dicarboxylic acids and are related to the low T_g and lower crosslinking density from those systems when compared with resins from DGEBA. The values found for the mechanical properties follow the same behavior that was observed for the swelling ratio in toluene and the crosslinking density (υ) deduced by dynamical mechanical analysis (DMA). In other words, an increase in properties is observed up to the molar ratio R =0.7 in the formulation following the decrease in tensile strength.

Some hypotheses are that values close to stoichiometric for the ESBOTAR system culminate in the precipitation or crystallization of domains rich in L-tartaric acid that do not participate in the esterification reaction and consequently reduce the density of cross-links, resulting in a decrease in the properties evaluated. The choice of the range of molar ratios to be studied in this work excludes the stoichiometric ratio (R= 1) once they macroscopically present phases rich in L-tartaric acid in the cured samples obtained.

Regardless of the reprocessing effect, after the 1st reprocessing cycle, a slight increase in the tensile strength is noticed, mostly for the molar ratio 0.5 and 0.8, which showed the lower performance for the pristine material. A possible explanation for this is that reprocessing conditions promoted an annealing in the material and consolidation in the structure. After the 3rd reprocessing, the tensile strength is quite close to the original range value (except for R = 0.8). Observing the elongation at break (strain) results, for all compositions is possible to observe an increase after the first and

second cycles of reprocessing followed by a decrease to the original patamar in the samples reprocessed 3 times. In general, the mechanical behavior did not decrease drastically after the reprocessing cycles, as expected, since Jie Li, *et al.* used a similar system (ESO and succinic and sebacic acid) and obtained values of tensile strength lower than 0.5 MPa for the reprocessed samples [22]. Another evidence that the average density of crosslinking did not decrease after the 3rd reprocessing is that the degree of swelling remained coherent with those presented for the pristine material (information provided in Table SM2 and Figure SM 22).

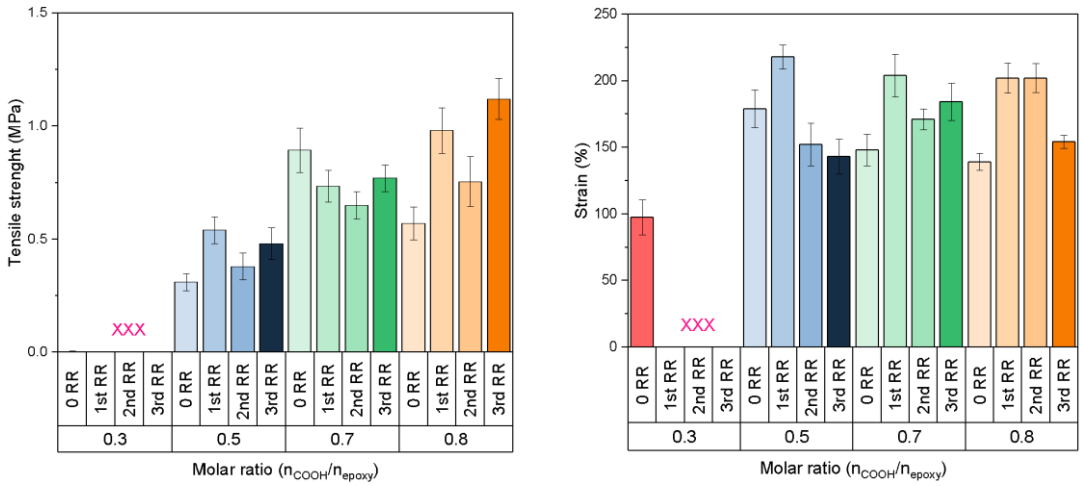

Figure 7 – Average maximum tensile strength (MPa) (left) and strain (%) (right) values from pristine (0 RR) and reprocessed (RR) ESBOTAR resins as a function of molar ratio.

Stress relaxation.

As already mentioned, the presence of extra hydroxyl functions distributed along the polymer chains can bring interesting properties especially when exchange reactions are targeted. To characterize the covalent exchange dynamic, stress relaxation experiments were performed and compared to a prototype material that does not contain the extra hydroxyl groups (from ESBO and succinic acid). Figure SM-23a shows the stress relaxation behavior at 160°C of ESBOTAR polymer networks prepared at various molar ratios. The characteristic relaxation time (τ^*) is defined as the time required for the material to relax to 1/e of its initial modulus, which is around 0.37 of (G/G_0). The relaxation profile recorded indicates a faster relaxation for the molar ratios

equal to 0.5 and 0.8, following the same behavior noticed in the gel content, swelling ratio, and thermal-mechanical properties.

Despite the molar ratio 0.7 presenting a longer relaxation time compared to 0.5 and 0.8, this formulation was chosen to calculate the activation energy, as it presented the higher tensile strength, which leads to the assumption that the ideal molar ratio is R = 0.7, once an increase above this value (as an example of R = 0.8) leads to a material which will have the same behavior of one with R= 0.5. Nevertheless, this performance is usually noticed and associated with the increase in the residual -OH concentration caused by either open ring reaction or in this case remaining -OH from tartaric acid. It has been reported that the transesterification reaction and consequently the stress relaxation rate increases with the concentration of -OH groups [21,40]. As can be seen, R = 0.3 does not relax instantaneously which is related to the lower crosslinking density and, consequently transesterification reactions are not favorable.

Figure 8a presents normalized curves for the evolution of relaxation modulus as a function of temperature in the 150°-190°C range. As can be seen, the stress relaxation rate increased with temperature, which corresponds to the increase in the transesterification reactions, as expected for a covalent adaptable network. A Kohlrausch-Williams-Watts model (stretched exponential equation) was used for fitting the data obtained and determining the relaxation times, since a Maxwell model (exponential decay) didn't provide a good fit. The R^2 and the β values obtained and the fitting parameters are presented in supplementary material (Table – SM1 and Figure SM-23b). The activation energy obtained was E_A = 88 kJ.mol^{-1} (R^2 = 0.98) which is the following values presented for CANs systems using epoxidized oils and carboxylic acids which vary from 58-155 kJ.mol^{-1} range, mostly intermediate by catalysts [42].

To prove the potential of tartaric acid, not only as a hardener but also its differential in the development of CANs from an epoxy-acid system without catalyst and completely bio-sourced, once again succinic acid was used as a reference since presents a similar chemical structure with the absence of -OH in the aliphatic chain. Following the same procedure used for the formulation and cure of ESBOTAR, a resin using succinic acid (ESBOSUC) with the molar ratio of 0.7 was developed and submitted to the stress relaxation test. Figure 8b presents the normalized curve obtained and is compared

with the ESBOTAR R=0.7. The relaxation time for ESBOSUC is τ*= 28150 s (7.8 h) in contrast with 10030 s (2.5 h) for ESBOTAR formulation, which confirms that the presence of OH groups from L-tartaric acid plays an important role in the transesterification reactions.

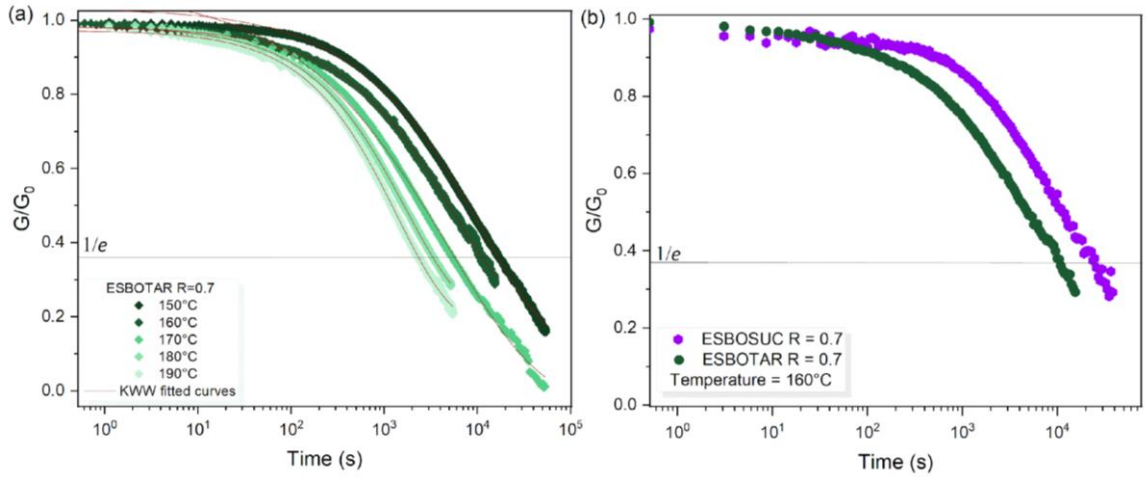

Figure 8 – (a) Normalized stress relaxation curve from ESBOTAR R = 0.7 system from 150-190°C fitted with Kohlrausch–Williams–Watts equation (KWW) and (b) Normalized stress relaxation curve from ESBOTAR and ESBOSUC system at 160°C.

Conclusion: In this work, a fully biobased epoxy system using epoxidized soybean oil (ESBO) and L-tartaric acid (TAR) as a eutectic hardener was successfully developed. We have demonstrated the successful synthesis of these materials with high degrees of crosslinking, efficient curing, and desirable elastomeric properties. The incorporation of TAR not only offers a renewable alternative to traditional petrochemical-based hardeners but also introduces extra hydroxyl groups along the polymer chains, enhancing reactivity and facilitating reprocessing without the need for exogenous catalysts. Our findings highlight the importance of optimizing the molar ratio between TAR and ESBO and presents an alternative to replacing petro-souced thermosets with desired mechanical, chemical, and thermal properties, given some perspectives for application in emerging areas such as biomedical, soft robotics and adhesives. Furthermore, stress relaxation experiments underscore the potential of the ESBOTAR system as a covalent adaptable network, with transesterification reactions driving material to reprocessability. Overall, this study offers insights into the design and

development of biobased epoxy systems with intrinsic reprocessability and recyclability without catalysts.

Acknowledgements

This work was supported by Institut Charles Gerhardt Montpellier (ICGM- France) in a collaboration with Conselho Nacional de Desenvolvimento de Cientifico e Tecnológico (CNPQ - Brazil) though the projects related to call N°26/2021 (Process n°: 200926/2022-5).

Experimental

Materials

Epoxidized soybean oil (ESBO) (EEW = 205 eq. g^{-1} and number of epoxy groups equal to 4.74) was kindly provided by Hobum Chemicals. L-tartaric acid (MW= 150 $g.mol^{-1}$, T_m= 174°C), toluene, and ethyl lactate were acquired from Sigma Aldrich. All the chemicals were used without further process of purification. The precise amount of epoxy groups in ESBO and its molecular weight were determined by ^1H NMR (Figure - SM1).

Methodology

Preparation of ethyl lactate and L-tartaric acid aqueous solution: To obtain a homogeneous and liquid solution, the stoichiometry amount of L-tartaric acid (TAR) (concerning ESBO) was dissolved in an aqueous solution of ethyl lactate (R = 0.2 ethyl lactate/H_2O). The mixture TAR/EL_{aq} (0.72 g/mL) was heated to 80°C and the dissolution of TAR occurred in 5-10 minutes.

Thermoset resin preparation: ESBOTAR epoxy samples with molar ratio -COOH/epoxide of 0.3, 0.5, 0.7, and 0.8 were prepared to evaluate the effect of molar ratio on the curing behavior and the thermal and mechanical properties of the thermoset. The samples were prepared as follows: the right amount of ESBO (25g) was heated to 60°C under a nitrogen atmosphere. After that, the solution of TAR/EL_{aq} was added to the ESBO and the solution was stirred for 30 minutes. Finally, one step of retro evaporation was added to remove the excess solvent. The samples were stored in a fridge to avoid any reactions before the curing process. The calculations are explained in the supplementary material.

Curing process: The curing process was done in a few steps. The samples were placed in a silicon mold and cured in an oven. First, the samples were placed in the oven at 65°C, and vacuum was applied for 15 minutes. Second, at room pressure, the temperature was raised to 105°C to enable the first curing reactions during 4h. Finally, the temperature was increased to 130°C and the curing process was carried out overnight to assure the maximum conversion.

Nuclear magnetic resonance (NMR): NMR samples were prepared with $CDCl_3$ as solvent and the analyses were performed using a Bruker Avance 400 MHz spectrometer at 25 °C. The epoxy ratio of oil was determined by hydrogen nuclear magnetic resonance (^{1}H NMR). The ^{1}H NMR spectra were recorded at 8 kHz for spectral width, 3 kHz for transmitter frequency offset, 4 seconds for acquisition time and 8 scans were performed. Calibrations were performed using residual solvent peak.

Spectroscopy (FT-IR): Spectra were recorded in a ThermoScientific (Nicolet IS50) spectrometer equipped with Golden-Specac heating cell ATR modulus. The data were collected using a 4 cm^{-1} resolution and 32 scans.

The degree of curing was also observed in terms of conversion (α, %) of epoxide groups comparing the uncured and cured samples and during the kinetic analysis at different times. According to the following equation adapted from Beer-Lambert Law [43].

$$\propto_{0\rightarrow t} = 1 - \frac{(A_E)_t}{(A_R)_0} \qquad \text{Eq-1}$$

Where A_E and A_R are the absorbance of peaks from the bands of epoxy at a time t and t=0, respectively.

Differential Scanning Calorimetry (DSC): Analyses were performed at a heating/cooling rate of 10°C.min^{-1} in nitrogen atmosphere using a NETZSCH 3500 Sirius analyzer. The calibration was performed using adamantane, biphenyl, indium, tin, bismuth and zinc standards. Nitrogen was used as the purge gas. Samples with approximately 10 mg were placed in high-pressure steel pans. The thermal properties were analyzed at 10 °C/min between -90 and 250 °C to observe the enthalpy reaction

in the first dynamic ramp and the glass transition temperature in the second dynamic ramp.

Thermogravimetric analysis (TGA): The thermal stability was evaluated using a TGA Q50 (TA instruments) and the measurements were performed with 10 mg of sample placed in an alumina crucible at a heating rate of 20°C/min from room temperature to 650°C under a nitrogen atmosphere.

Gel content (%) and chemical resistance: The gel fraction and swelling ratio of samples were determined in a 10mL vial by covering vacuum-dried samples with a mass of 350 mg with 7 ml of THF and toluene (25°C) and DMF (60°C) (Supplementary material material). Samples were kept for 48h after which the samples were removed from the vial and dried in a vacuum oven until a constant weight was reached. The gel fraction was calculated according to the following equation:

$$Gel\ fraction\ (\%) = \frac{m_d}{m_i} \times 100 \qquad \text{Eq-2}$$

where m_d and m_i were the dry and initial masses, respectively.

The chemical resistance was evaluated in acid and basic medium and consisted in the immersion of samples (cylindric discs with approximately 350 mg) in a 1M HCl and 1M NaOH solutions for 1 week.

Size Exclusion Chromatography: SEC was recorded using a triple-detection GPC from Agilent Technologies with its corresponding Agilent software, dedicated to multidetector GPC calculation. The system used two PL1113-6300 ResiPore 300 × 7.5 mm columns with THF as the eluent with a flow rate of 1 mL·min^{-1}. The detector was a 390-LC PL0390-0601 refractive index detector. The entire SEC-HPLC system was thermostated at 35 ◦C. Polymethylmethacrylate (PMMA) standards were used for calibration between 540 and 2,210,000 g·mol^{-1}. Samples were prepared by diluting 0.1 mL aliquots of EMO and EMOTAR samples in 1 mL THF.

Swelling ratio (%): The swelling ratio (S_r) was determined according to Equation-3 and the results are shown as absorbed solvent content expressed in percentage units.

Specimens with initial weight (W_i), approximately 350 mg, were immersed in 50 mL of toluene at room temperature and in DMF at 60°C for 48h (Supplementary material). Then, the specimens were gently dried to remove solvent excess and the final weights (W_f) were recorded.

$$Swelling\ ratio\ (S_r\ in\ \%) = \frac{W_f - W_i}{W_i}\ x\ 100$$ Eq-3

Toluene was used as major solvent for swelling ratio based in previous works that related to development of bio based resins using epoxidized vegetable oils [15].

Dynamic Mechanical Analyzer (DMA): Analyses were carried out on Metravib DMA 25 with Dynatest 6.8 software. Uniaxial stretching of samples (30 x 7 x 2 mm^3) was performed using heating at a rate of 3°C.min^{-1} from −50 °C to 150 °C, keeping the frequency at 1 Hz.

The data was used to calculate the crosslinking density (υ in $g.mol^{-1}$) was determined using Flory's theory of rubber elasticity [44] as described in the following equation:

$$\upsilon = \frac{E'}{3RT}$$

Eq-4

And, considering that the density (ρ) does not change significantly as a function of the molar ratio then, we can assume that:

$$M_c \equiv \frac{1}{\upsilon}$$

where E' (Pa) is the storage modulus in the rubbery region at a given temperature T (T =T_g + 50) in Kelvin R is the gas constant (8.314 $m^3.Pa.K^{-1}.mol^{-1}$) and M_c is the molecular weight between two crosslinked dots (g/mol).

Tensile tests: Tensile tests were performed on a Instron 3360 with a load cell of 100 kN at a deformation rate of 10 mm min^{-1}. At least five different dog-bone specimens with 35 mm width, 25 mm gauge length and ≈ 2 mm thickness were tested.

Reprocessing: the material was cut into small pieces (dimensions around 1 × 1 × 1 mm^3)

and then pressed between two stainless steel plates covered with PTFE sheets overnight (around 15h) at 145 °C under a 4tons load using a Carver 3960 manual heating press. The reprocessing protocol takes in considerations the influence of those parameters in the final material as proposed in some works in the literature [41,42].

Rheology: Stress relaxation was performed on a Rheometer Anton Parr equipped with a sandblasted 8 mm plane-plane geometry. The viscoelastic regime was determined by

strain-sweep experiment at the desired temperatures. A 1% strain was applied on a disk-shaped sample with an 8 mm diameter and 1.8 mm thickness, and the relaxation modulus (G_0) was monitored as a function of time.

The characteristic relaxation times recorded were used to trace an Arrhenius-type curve using the following equation:

$$ln\,\tau^* = \frac{E_a}{RT} - ln\,A \qquad \text{Eq-5}$$

References

[1] M.R. Vengatesan, A.M. Varghese, V. Mittal, Thermal properties of thermoset polymers, 2nd ed., Elsevier Ltd., 2018. https://doi.org/10.1016/B978-0-08-101021-1.00003-4.

[2] D. Montarnal, M. Capelot, F. Tournilhac, L. Leibler, Silica-like malleable materials from permanent organic networks, Science (80-.). 334 (2011) 965–968. https://doi.org/10.1126/science.1212648.

[3] Z. Ma, Y. Wang, J. Zhu, J. Yu, Z. Hu, Bio-based epoxy vitrimers: Reprocessibility, controllable shape memory, and degradability, J. Polym. Sci. Part A Polym. Chem. 55 (2017) 1790–1799. https://doi.org/10.1002/pola.28544.

[4] Y. Tao, X. Liang, J. Zhang, I.M. Lei, J. Liu, Polyurethane vitrimers: Chemistry, properties and applications, J. Polym. Sci. 61 (2022) 22. https://doi.org/10.1002/pol.20220625.

[5] K. Yu, P. Taynton, W. Zhang, M.L. Dunn, H.J. Qi, Reprocessing and recycling of thermosetting polymers based on bond exchange reactions, RSC Adv. 4 (2014) 10108–10117. https://doi.org/10.1039/c3ra47438k.

[6] S. Kumar, S. Krishnan, S.K. Samal, S. Mohanty, S.K. Nayak, Toughening of Petroleum Based (DGEBA) Epoxy Resins with Various Renewable Resources Based Flexible Chains for High Performance Applications: A Review, Ind. Eng. Chem. Res. 57 (2018) 2711–2726. https://doi.org/10.1021/acs.iecr.7b04495.

[7] A.M. Sienkiewicz, P. Czub, The unique activity of catalyst in the epoxidation of soybean oil and following reaction of epoxidized product with bisphenol A, Ind. Crops Prod. 83 (2016) 755–773. https://doi.org/10.1016/j.indcrop.2015.11.071.

[8] FAO, USDA-grain: world markets and trade-2023, USDA-Grain World Mark. Trade. 22 (2023) 22–43. https://www.statista.com/statistics/263977/world-grain-production-by-type/.

[9] United States Department of Agriculture, Oilseeds: Diverging Trends for U.S. Soybean and Soybean Meal Exports in 2023, (2024) 1–39.

https://public.govdelivery.com/accounts/USDAFAS/subscriber/new.

[10] W. Li, X.H. Kong, M. Ruan, F.M. Ma, Y.F. Jiang, M.Z. Liu, Y. Chen, X.H. Zuo, Green waxes, adhesives and lubricants., Philos. Trans. A. Math. Phys. Eng. Sci. 368 (2010) 4869–4890. https://doi.org/10.1098/rsta.2010.0197.

[11] T. Vidil, A. Llevot, Fully Biobased Vitrimers: Future Direction toward Sustainable Cross-Linked Polymers, Macromol. Chem. Phys. 223 (2022) 1–21. https://doi.org/10.1002/macp.202100494.

[12] M. Galià, L.M. de Espinosa, J.C. Ronda, G. Lligadas, V. Cádiz, Vegetable oil-based thermosetting polymers, Eur. J. Lipid Sci. Technol. 112 (2010) 87–96. https://doi.org/10.1002/ejlt.200900096.

[13] S. Malburet, C. Di Mauro, C. Noè, A. Mija, M. Sangermano, A. Graillot, Sustainable access to fully biobased epoxidized vegetable oil thermoset materials prepared by thermal or UV-cationic processes, RSC Adv. 10 (2020) 41954–41966. https://doi.org/10.1039/d0ra07682a.

[14] M. Pawar, A. Kadam, O. Yemul, V. Thamke, K. Kodam, Biodegradable bioepoxy resins based on epoxidized natural oil (cottonseed & algae) cured with citric and tartaric acids through solution polymerization: A renewable approach, Ind. Crops Prod. 89 (2016) 434–447. https://doi.org/10.1016/j.indcrop.2016.05.025.

[15] C. Di Mauro, S. Malburet, A. Genua, A. Graillot, A. Mija, Sustainable Series of New Epoxidized Vegetable Oil-Based Thermosets with Chemical Recycling Properties, Biomacromolecules. 21 (2020) 3923–3935. https://doi.org/10.1021/acs.biomac.0c01059.

[16] T.S. Omonov, J.M. Curtis, Biobased epoxy resin from canola oil, J. Appl. Polym. Sci. 131 (2014) 1–9. https://doi.org/10.1002/app.40142.

[17] A. Kadam, M. Pawar, O. Yemul, V. Thamke, K. Kodam, Biodegradable biobased epoxy resin from karanja oil, Polymer (Guildf). 72 (2015) 82–92. https://doi.org/10.1016/j.polymer.2015.07.002.

[18] A. Anusic, Y. Blößl, G. Oreski, K. Resch-Fauster, High-performance thermoset

with 100 % bio-based carbon content, Polym. Degrad. Stab. 181 (2020) 109284. https://doi.org/10.1016/j.polymdegradstab.2020.109284.

[19] J. Verduyckt, D.E. De Vos, Highly selective one-step dehydration, decarboxylation and hydrogenation of citric acid to methylsuccinic acid, Chem. Sci. 8 (2017) 2616–2620. https://doi.org/10.1039/c6sc04541c.

[20] S. Ma, D.C. Webster, Naturally Occurring Acids as Cross-Linkers To Yield VOC-Free, High-Performance, Fully Bio-Based, Degradable Thermosets, Macromolecules. 48 (2015) 7127–7137. https://doi.org/10.1021/acs.macromol.5b01923.

[21] F.I. Altuna, V. Pettarin, R.J.J. Williams, Self-healable polymer networks based on the cross-linking of epoxidised soybean oil by an aqueous citric acid solution, Green Chem. 15 (2013) 3360–3366. https://doi.org/10.1039/c3gc41384e.

[22] J. Li, S. Zhang, B. Ju, Soft, fully bio-based poly-hydroxyl thermosets based on catalyst-free transesterification with decent re-processability, J. Appl. Polym. Sci. 139 (2022) 1–12. https://doi.org/10.1002/app.52676.

[23] S.K. Sahoo, V. Khandelwal, G. Manik, Development of completely bio-based epoxy networks derived from epoxidized linseed and castor oil cured with citric acid, Polym. Adv. Technol. 29 (2018) 2080–2090. https://doi.org/10.1002/pat.4316.

[24] J. Tellers, P. Willems, B. Tjeerdsma, N. Guigo, N. Sbirrazzuoli, Eutectic hardener from food-based chemicals to obtain fully bio-based and durable thermosets, Green Chem. 22 (2020) 3104–3110. https://doi.org/10.1039/d0gc00311e.

[25] J. Tellers, M. Jamali, P. Willems, B. Tjeerdsma, N. Sbirrazzuoli, N. Guigo, Cross-linking behavior of eutectic hardeners from natural acid mixtures, Green Chem. 23 (2021) 536–545. https://doi.org/10.1039/d0gc03172k.

[26] R. Devesa-rey, X. Vecino, J.L. Varela-alende, M.T. Barral, J.M. Cruz, A.B. Moldes, Valorization of winery waste vs . the costs of not recycling, Waste Manag. 31 (2011) 2327–2335. https://doi.org/10.1016/j.wasman.2011.06.001.

[27] K.N. Kontogiannopoulos, S.I. Patsios, A.J. Karabelas, Tartaric acid recovery from winery lees using cation exchange resin : Optimization by Response Surface Methodology, Sep. Purif. Technol. 165 (2016) 32–41. https://doi.org/10.1016/j.seppur.2016.03.040.

[28] M.A. Bustamante, R. Moral, C. Paredes, A. Pérez-Espinosa, J. Moreno-Caselles, M.D. Pérez-Murcia, Agrochemical characterisation of the solid by-products and residues from the winery and distillery industry, Waste Manag. 28 (2008) 372–380. https://doi.org/10.1016/j.wasman.2007.01.013.

[29] L. Gong, S. Wang, J. Hu, H. Feng, L. Zhang, J. Dai, X. Liu, A novel bio-based degradable, reinforced vitrimer regulated by intramolecular hydrogen bonding, Prog. Org. Coatings. 175 (2023) 107384. https://doi.org/10.1016/j.porgcoat.2022.107384.

[30] C. Bakkali-Hassani, P. Edera, J. Langenbach, Q.A. Poutrel, S. Norvez, M. Gresil, F. Tournilhac, Epoxy Vitrimer Materials by Lipase-Catalyzed Network Formation and Exchange Reactions, ACS Macro Lett. 12 (2023) 338–343. https://doi.org/10.1021/acsmacrolett.2c00715.

[31] C. Bakkali-Hassani, Q.A. Poutrel, J. Langenbach, S. Chappuis, J.J. Blaker, M. Gresil, F. Tournilhac, Lipase-Catalyzed Epoxy-Acid Addition and Transesterification: From Model Molecule Studies to Network Build-Up, Biomacromolecules. 22 (2021) 4544–4551. https://doi.org/10.1021/acs.biomac.1c00820.

[32] Z. Yan, Z. Ma, J. Deng, G. Luo, Mechanism and kinetics of epoxide ring-opening with carboxylic acids catalyzed by the corresponding carboxylates, Chem. Eng. Sci. 242 (2021) 116746. https://doi.org/10.1016/j.ces.2021.116746.

[33] C. Menager, N. Guigo, L. Vincent, N. Sbirrazzuoli, Polymerization kinetic pathways of epoxidized linseed oil with aliphatic bio-based dicarboxylic acids, J. Polym. Sci. 58 (2020) 1717–1727. https://doi.org/10.1002/pol.20200118.

[34] F. Jaillet, M. Desroches, R. Auvergne, B. Boutevin, S. Caillol, New biobased carboxylic acid hardeners for epoxy resins, Eur. J. Lipid Sci. Technol. 115 (2013)

698–708. https://doi.org/10.1002/ejlt.201200363.

[35] J.A. Arcos-Casarrubias, H. Vázquez-Torres, J.A. Granados-Olvera, A.J. Cedeño, J.M. Cervantes-Uc, Viscoelastic behavior and toughness of the DGEBA epoxy resin with 1,2-diaminocyclohexane: effect of functionalized poly(dimethylsiloxane), diglycidyl ether, PDMS-DGE, pre-reacted with 1,2-diaminocyclohexane, Polym. Bull. 79 (2022) 2871–2901. https://doi.org/10.1007/s00289-021-03607-y.

[36] A.E. Gerbase, C.L. Petzhold, A.P.O. Costa, Dynamic mechanical and thermal behavior of epoxy resins based on soybean oil, JAOCS, J. Am. Oil Chem. Soc. 79 (2002) 797–802. https://doi.org/10.1007/s11746-002-0561-z.

[37] C. Hood, S.M. Ghazani, A.G. Marangoni, E. Pensini, Flexible polymeric biomaterials from epoxidized soybean oil, epoxidized oleic acid, and citric acid as both a hardener and acid catalyst, J. Appl. Polym. Sci. 139 (2022) 9. https://doi.org/10.1002/app.53011.

[38] E. Mazzon, P. Guigues, J.P. Habas, Biobased structural epoxy foams derived from plant-oil: Formulation, manufacturing and characterization, Ind. Crops Prod. 144 (2020) 111994. https://doi.org/10.1016/j.indcrop.2019.111994.

[39] P. Ortiz, M. Wiekamp, R. Vendamme, W. Eevers, Bio-based epoxy resins from biorefinery by-products, BioResources. 14 (2019) 3200–3209. https://doi.org/10.15376/biores.14.2.3200-3209.

[40] M. Capelot, D. Montarnal, F. Tournilhac, L. Leibler, Metal-catalyzed transesterification for healing and assembling of thermosets, J. Am. Chem. Soc. 134 (2012) 7664–7667. https://doi.org/10.1021/ja302894k.

[41] S. Chappuis, P. Edera, M. Cloitre, F. Tournilhac, Enriching an Exchangeable Network with One of Its Components: The Key to High- TgEpoxy Vitrimers with Accelerated Relaxation, Macromolecules. 55 (2022) 6982–6991. https://doi.org/10.1021/acs.macromol.2c01005.

[42] A. Kumar, L.A. Connal, Biobased Transesterification Vitrimers, Macromol. Rapid Commun. 44 (2023) 1–21. https://doi.org/10.1002/marc.202200892.

[43] M.C. Finzel, J. Delong, M.C. Hawley, Effect of stoichiometry and diffusion on an epoxy/amine reaction mechanism, J. Polym. Sci. Part A Polym. Chem. 33 (1995) 673–689. https://doi.org/10.1002/pola.1995.080330409.

[44] P.J. Flory, Principles of polymer chemistry, Cornell University Press, 1953.

[45] H. Zhang, J. Cui, G. Hu, B. Zhang, Recycling strategies for vitrimers, Int. J. Smart Nano Mater. 13 (2022) 367–390. https://doi.org/10.1080/19475411.2022.2087785.

[46] H. Li, B. Zhang, K. Yu, C. Yuan, C. Zhou, M.L. Dunn, H.J. Qi, Q. Shi, Q.H. Wei, J. Liu, Q. Ge, Influence of treating parameters on thermomechanical properties of recycled epoxy-acid vitrimers, Soft Matter. 16 (2020) 1668–1677. https://doi.org/10.1039/c9sm02220a.